On-Chip Drop-to-Drop Liquid Microextraction Coupled with Real-Time Concentration Monitoring Technique

ARTICLE *in* ANALYTICAL CHEMISTRY · FEBRUARY 2011

Impact Factor: 5.64 · DOI: 10.1021/ac102716s · Source: PubMed

5 AUTHORS, INCLUDING:

Pavithra A L Wijethunga
University of Texas at Arlington
8 PUBLICATIONS **75** CITATIONS
SEE PROFILE

Yasith Nanayakkara
U.S. Food and Drug Administration
12 PUBLICATIONS **159** CITATIONS
SEE PROFILE

Daniel W. Armstrong
University of Texas at Arlington
677 PUBLICATIONS **24,379** CITATIONS
SEE PROFILE

Hyejin Moon
University of Texas at Arlington
40 PUBLICATIONS **2,725** CITATIONS
SEE PROFILE

analytical chemistry

ARTICLE

pubs.acs.org/ac

On-Chip Drop-to-Drop Liquid Microextraction Coupled with Real-Time Concentration Monitoring Technique

Pavithra A. L. Wijethunga,[†] Yasith S. Nanayakkara,[‡] Praveen Kunchala,[†] Daniel W. Armstrong,[‡] and Hyejin Moon*[,†]

[†]Department of Mechanical and Aerospace Engineering, and [‡]Department of Chemistry and Biochemistry, The University of Texas at Arlington, Arlington, Texas 76019, United States

Supporting Information

ABSTRACT: This paper demonstrates a novel drop-to-drop liquid−liquid microextraction (DTD-LLME) device, which is based on an electrowetting on dielectric (EWOD) digital microfluidic chip. Droplets of two immiscible liquids, one of which is an ionic liquid, are formed in nanoliter volumes, driven along electrodes, merged and mixed for extraction, and finally separated upon the completion of the extraction process. All the steps are carried out on a microfluidic chip using combined electrowetting and dielectrophoretic forces, which act on the droplet upon the application of electric potential. Specially, the phase separation of two immiscible nanoliter-scale liquid drops was achieved for the first time on an EWOD digital microfluidic chip. To study the on-chip extraction kinetics, an image-based concentration measurement technique with suitable color parameters was studied and compared with the typical UV absorption based technique. Finally, the effect of applied ac voltage frequency on the extraction kinetics was studied. The observations on DTD-LLME, particularly phase separation, are discussed. The image-based method was found to be applicable for precise concentration measurements with the right choice of the color parameter. Results from experiments on finding the frequency dependence on extraction kinetics demonstrate that the application of higher frequencies can be a factor in accelerating the extraction on the proposed microextraction device.

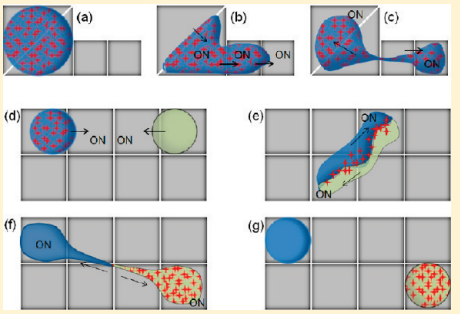

Liquid−liquid extraction is one of the most widely used sample pretreatment techniques in basic sciences. Traditional liquid−liquid extraction methods can consume large quantities of organic solvents, which lead to environmentally hazardous waste products. In addition, typically liquid−liquid extraction can be time-consuming and require trained personnel, which elevates cost for unitary or multiplexed industrial procedures.[1] To minimize these drawbacks, miniaturization methods, such as liquid-phase microextraction and single-drop microextraction, were proposed.[2−4] Despite recent developments, pros and cons of different versions of microextraction platforms reveal the need for continuous innovation toward integrated analytical systems.[5] For instance, an extraction device that can facilitate multiplexing or high-throughput operation has never been considered. Thus, we introduce a new drop-to-drop liquid−liquid microextraction (DTD-LLME) approach, a lab-on-chip method, which can easily handle parallel multiple extraction processes. The device is based on electrowetting on dielectric (EWOD) digital microfluidics, where both sample and extractant are handled in micro/nano droplet formats. The proposed device provided enhanced performance because it combines the use of ionic liquids as solvents and the utility of an EWOD digital microfluidic, which can be operated via remote computer programming.

EWOD digital microfluidic is a new type of microfluidic lab-on-a-chip system in which liquid drops are created and actuated by application of digitized voltages.[6] The interest in EWOD digital microfluidic devices has increased tremendously given their versatility over traditional microfluidic devices. They have been used to perform sample preparations for matrix-assisted laser desorption ionization mass spectrometry for protein analysis as well as to provide an efficient platform for chemical reactions.[7−12] Hence, their potential to be integrated into micro total analysis systems is apparent. Previous efforts on EWOD digital microfluidic demonstrated not only the advantage of handling liquids in small volumes with high accuracy but also its capability to perform various multiplexing processes which empowers an EWOD device to be an advantageous platform for high-throughput screening processes. Hence, identifying, developing, and analyzing microextractions on EWOD digital microfluidic platforms would be beneficial in achieving such total analysis systems. Recently, Abdelgawad et al. reported a liquid−liquid micro extraction process on a specific nonplanar EWOD platform.[13] Although they showed the purification of a contaminated DNA droplet by driving it back and forth into a pool of water-immiscible extractant, the device needs to be partially immersed into the extractant pool. Clearly, a microextraction device where both donor and extractant are handled in terms of micro/nanoscale droplets would be preferred. Such a device would provide a better control over the donor-to-extractant ratio, comparatively lower extractant and donor consumption, and a much simpler device configuration and operation. As will be shown,

Received: October 19, 2010
Accepted: January 5, 2011
Published: February 04, 2011

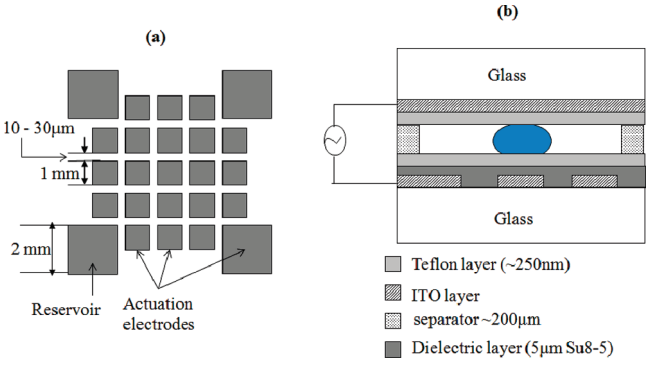

Figure 1. (a) Top view of the working area of the EWOD device and (b) cross-sectional view of the experimental arrangement.

this can be easily achieved by replacing the organic solvents in the extraction process with room-temperature ionic liquids.

Ionic liquids (ILs) are organic salts which are liquids at ambient conditions. In comparison to other liquids, ILs have unique properties such as, negligible evaporation, higher thermal stabilities, and tunable chemical and physical properties.[14] Because of these advantages ILs are used in many chemical applications including liquid−liquid extractions.[15,16] In previous studies ILs were used to selectively extract proteins and other analytes in macroscale.[17,18] Also some ILs were used in microscale in solid-phase microextraction.[19−21]

In this paper, an EWOD digital microfluidic device was used to demonstrate the first DTD-LLME of an acidic dye (solute) from an aqueous droplet (donor) to an IL droplet (extractant). On the EWOD digital microfluidic platform, donor and extractant are dispensed as ~200 nL droplets and extraction takes places at the interface between these nanodroplets. Four major steps for a DTD-LLME (e.g., dispensing droplets, moving and merging, mixing to effect extraction, and separating extractant phase from donor phase) are demonstrated experimentally. To quantify the extraction performance and kinetics, the device was then combined with an image-based concentration monitoring technique. A conventional UV absorbance based measurement technique was also applied for comparison purpose. Further, we studied the potential contribution of the applied ac voltage frequency in enhancing the extraction performance on the proposed device. The study on frequency dependence was encouraged by the recent findings of surface oscillations and internal flow patterns that occur inside droplets under ac electrowetting.[14,22−26] Finally, several important experimental observations, the results, and future directions will be discussed.

EXPERIMENTAL SECTION

EWOD Microextraction Device Fabrication. DTD-LLME devices were fabricated at the University of Texas at Arlington Nanofabrication facility. First, ITO (indium tin oxide) coated glass wafers (Delta Technologies Ltd., Stillwater, MN) were cleaned in piranha solution for 15 min and dehydrated at 175 °C. The substrates were primed by spin-coating of hexamethyldisilazane (3000 rpm, 30 s), baked on a hot plate (150 °C for 90 s), and then spin-coated with Shipley S1813 photoresist (4000 rpm, 30 s, 1.3 μm). Substrates were prebaked on a hot plate (150 °C for 1 min) and exposed through a photomask (Figure 1a) using an aligner. Then the substrates were developed in MF319 (50 s) and then postbaked on a hot plate (115 °C, 2 min). After photolithography, substrates were immersed in ITO etchant (20 wt % HCl, 5 wt % HNO_3, 75 wt % H_2O, or 8:1:15 vol % $HCl/HNO_3/H_2O$) at 55 °C for 2.5 min to pattern the ITO layer to realize actuation electrodes.

The wafer is then diced, and the remaining photoresist was stripped using stripper (ALEG-355). While the contact pads on each chip were covered, negative photoresist SU8-5 was spin-coated on the surface at 3000 rpm for 30 s to obtain a 5 μm layer of SU8-5. Substrates are prebaked at 95 °C for 3 min before exposing to UV on the aligner without a mask for 6 s. Post-exposure bake was done at 175 °C for 8 min. Cleaned chip surfaces were spin-coated with Teflon-AF (2000 rpm, 60 s, 250 nm) to provide hydrophobic surfaces and then annealed at 330 °C for a few hours to increase surface uniformity.

The patterned substrate design is shown in Figure 1a which shows the layout of the device design which has 1 mm × 1 mm actuation electrodes with an interelectrode gap of 10−30 μm and 2 mm × 2 mm reservoir electrodes. Each device was assembled with an ITO-coated glass substrate on the top, which forms a contiguous electrode, and a patterned substrate at the bottom separated by a spacer (~200 μm thick) as shown in Figure 1b, a cross-sectional view of the EWOD device.

Solute, Donor, and Extractant. To demonstrate the microextraction device, we selected an organic dye, namely, acid green 25, chemical formula $C_{28}H_{20}N_2Na_2O_8S_2$ (samples were provided by Organic Dyestuffs Corporation), as the solute. Water and a water-immiscible IL, 1-butyl-3-methylimidazolium hexafluorophosphate ([bmim][PF_6]), were selected as donor and extractant phases, respectively. The IL was prepared as previously reported.[14,27] Several studies have reported the extraction performance as well as the extraction mechanisms of [bmim][PF_6] in extracting analytes, such as Hg^{2+}, Cd^{2+}, and strontium ions.[27−31] Acid green 25 is soluble in both water and [bmim][PF_6] and has a desired distribution ratio for the extraction process. Dye aqueous solution with a concentration 1 g/L was used as donor solution.

Drop-to-Drop Microextraction Process. An electric potential (80−100 V_{rms}) is applied between the top and a bottom electrodes with 1 kHz frequency to dispense and move donor and extractant drops. (The experimental setup is shown in Supporting Information Figure S-1.) The required ac voltage signal was generated by a function generator (Agilent 33220A) and amplified by a power amplifier (Trek Inc. BZD350). Input voltage can be applied to several electrodes in a desired pattern through a control circuit and a data acquisition system (NI DAQ USB 6509), which is controlled by an interfacing software (NI Labview 8.5). Droplet actuation is monitored and recorded using a digital microscope system (HIROX KH 1300).

Figure 2 illustrates the entire procedure of the DTD-LLME on an EWOD chip. With the use of a micropipet, each drop of donor and extractant was placed on two reservoirs of the bottom plate of the microfluidic device (Figure 2a). Drops were sandwiched between the top and bottom electrode plates as shown in Figure 1b.

First, the sample droplets are dispensed from the reservoir drop by activating an electrode adjacent to the reservoir electrode, to pull a small liquid volume onto it (Figure 2b). Then the two end electrodes are activated as shown in Figure 2c. Consequently, the electrowetting forces create a neck between the two activated electrodes and the liquid instability at the neck finally forms a droplet. Dispensed droplets are further actuated along the electrode paths simply by activating the consecutive electrodes one after the other. Merging donor and extractant droplets is done by bringing two droplets onto a successive electrode (Figure 2d). Then the merged donor and extractant droplets are mixed by systematically activating

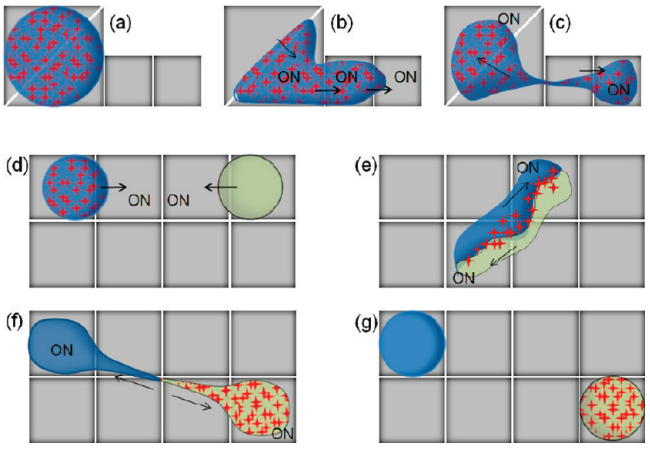

Figure 2. Unit operation of DTD-LLME on an EWOD chip. The electrodes are not activated unless they are labeled as "ON". The arrows show the direction of droplet flow. (a) Donor (blue) solution containing the solute (red) is placed on the reservoir electrodes, (b) driving the solution toward an electrode to break a droplet, (c) forming a neck and forming a droplet, (d) driving the donor and extractant (green) drops to merge, (e) mixing the merged droplets to fasten the extraction, solutes diffuse from donor to the extractant, (f) separating the two phases once the extraction is completed, and (g) donor (without solute) and extractant (with solute) after the successful phase separation.

electrodes (Figure 2e). Once the extraction is completed, phase separation is also done by driving the two phases onto two separate opposite electrodes as shown in Figure 2f.

The extraction kinetics can be observed real time through the digital microscope. Even though the UV spectrophotometer can be used for concentration measurements, image processing based concentration techniques are still advantageous for experiments considering the convenience in obtaining real-time concentration measurements. Therefore, after comparing the calibration curves for both the techniques, an image processing method was used for measuring extraction kinetics.

Concentration Measurement Technique for the Device. Two methods were studied to measure dye concentrations of the sandwiched droplets. First, we calibrated the UV absorption based technique for comparison. As the setup shown in Supporting Information Figure S-1a, a separate device holder integrated with a UV spectrophotometer was used for the UV absorption technique. Once the device is placed on the setup, the droplet sandwiched on the device can be aligned with the 200 μm diameter fiber optic (P200-2-UV−vis). Acid green 25 has the optimal absorption at 645 nm wavelength; hence an LED with 650 nm dominant wavelength was used as the light source.

Second, an image-based concentration method, which is based on the variation of solution color or gray level intensities at varying concentrations, was implemented. Typically, the perceived color can be different from true color (chromaticity) depending on the illumination and/or luminance conditions, such as light source. To minimize possible effects due to illumination changes from one experiment to another, color models that are designed to separate chromaticity from illumination are often used for color-based measurements. There exist several color models with different properties to represent color. Here we compare the use of three such color models for measuring on-chip real-time concentration of reagents. The three color models are RGB (red, green, blue), HSI (hue, saturation, illumination), and CIELab (Commission Internationale de L'Éclairage defined lightness, and *a*, *b* colors).[32] In order to study the suitable color model for concentration measurements, the responses of each color model parameter to the change in concentration of donor solution were compared. MATLAB software was used to select a region of interest from the image and to extract the averaged measurement over the region. The color measurements were calculated as the change of parameter value with respect to the reference (water) parameter value.

The previously described image-based technique was used for real-time concentration monitoring. We captured images each minute after the extraction starts, up to the duration of 10 min. Instead of measuring the concentration of analyte in the extractant, the change in concentration in the donor was used as a measure of extraction kinetics. The reasons are (i) during the extraction process, the color change of aqueous solution was almost homogeneous throughout the droplet, which is in contrast to the color distribution in the extractant ([bmim][PF_6]) droplet and (ii) extracted dye particles are mostly concentrated at the liquid−liquid interface.

RESULTS AND DISCUSSION

Droplet Generation, Extraction, and Separation. The microextraction device was used (i) to form donor and extractant droplets of about 200 nL in volume, (ii) to successfully extract $C_{28}H_{20}N_2Na_2O_8S_2$ dye molecules from droplets of aqueous solution to the extractant [bmim][PF_6] droplets, and (iii) to completely separate the two liquid phases from each other. The sequential snapshots obtained from a recorded experiment are presented in Figure 3.

It was comparatively easier to form a droplet from [bmim][PF_6] reservoirs and drive it smoothly along electrodes compared to actuating the aqueous dye solution. Particularly, the higher the dye concentration, the higher was the donor's resistance to move. A study on the forces that influence the liquid drop actuation may explain this observation. When the forces contributing to the droplet actuation are considered, both electrowetting forces as well as dielectrophoretic forces can be dominant depending on the liquid's properties.[33]

When the liquid acts like a conductor the electrowetting force is dominant, whereas when the liquid acts as a dielectric material, then the dielectrophoretic force is dominant. Liquid behavior, that is, whether it acts as a conductor or a capacitor, is affected by the ac frequency.[34] At low frequencies, the aqueous drop can be considered as a conductor. Hence, the electrowetting force is the dominant force for droplet actuation. Therefore, we experimentally investigated the effect of acid green 25 concentrations on the induced electrowetting force in order to understand the resistance to actuate. According to the fundamental equation of EWOD, the electrowetting force is proportional to the apparent contact angle change.[35] We measured the apparent contact angle of sessile drops (5 μL) at different dye concentrations, and the result is shown in Supporting Information Figure S-2a. According to the results, the range of apparent contact angle is increased when the dye concentration is increased. This result does not explain our observation of resistance to movement at higher concentrations. However, in addition to apparent contact angle change, the reversibility also is important for movability.

Reversibility is the ability to bring the electrowetted contact angle back to the initial position upon the removal of applied voltage. Lower reversibility may keep the electrowetting force constant after the first few applications of voltage, regardless of whether a voltage is applied or not. Then the droplet cannot be

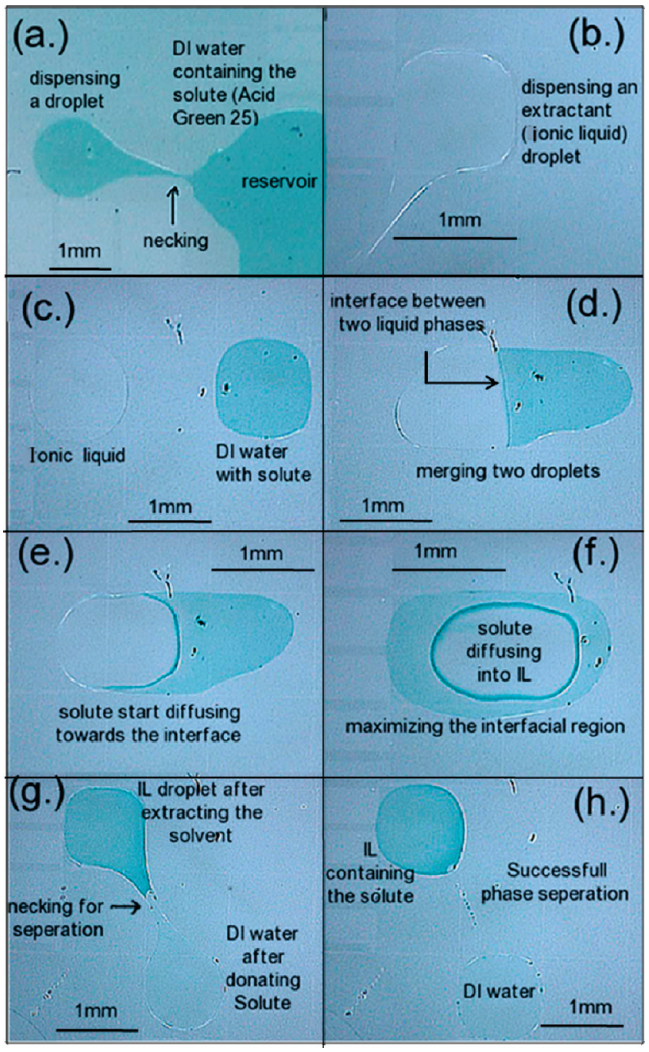

Figure 3. Sequential snapshots from the video record of the extraction experiment demonstrating different stages of the DTD-LLME process: dispensing a droplet of (a) aqueous dye (acid green 25) solution and (b) ionic liquid (IL) droplets from their reservoir drop; (c) the two droplets are about to be brought into contact; (d) merging two droplets; (e) diffusion of dye from aqueous solution to the IL; (f) increased interface between the two droplets by making the aqueous droplet be surrounded by the IL droplet; (g) create necking to separate the extractant phase from the donor phase; (h) extractant (IL) in blue and the colorless DI water droplet after the complete separation.

controlled or actuated by activating electrodes. An experiment to test the reversibility at different concentrations of donor solution was carried out. First, the voltage was applied to the sessile drop (ON position) and contact angle was recorded, then the voltage was switched off (OFF position), and after 5 s the contact angle was recorded again. This procedure was repeated for 5 V increments until the contact angle was saturated. The result plotted in Supporting Information Figure S-2b shows that the apparent contact angle of the water drop follows the applied voltage pattern. There, the contact angles achieved at all voltage OFF (0 V) conditions were approximately similar. However, the contact angle response of the donor solution to the OFF voltage (0 V) conditions was getting weaker as the concentration increased; thus, less contact angle changes between ON and OFF voltages were observed. This reduced reversibility explains the resistant to actuation at higher concentrations of acid green 25, and it could be due to surface adsorption of solutes. This phenomena has been observed also for biofluids on EWOD devices.[36] There are several proven solutions to the adsorption issue which will not limit the use of the microextraction device.[36−38] As an example, we tested one such solution,[37] adding a low concentration of Pluronic F68 (0.1% w/v Pluronic F68, Sigma-Aldrich, St. Louis, MO) matrix. This significantly improved the reversibility of the 1 g/L concentrated donor solution as shown in Supporting Information Figure S-2c.

Once the formed droplets are driven along the electrode and merged, the combined two phases can be mixed by driving them back and forth to enhance the extraction process. This was observed to be a smooth operation even when donor solutions showed resistance to move before the droplets were merged. During the extraction process, it was clearly observed that the donor phase become increasingly mobile as the analyte concentration decreased. While mixing, an interesting phase phenomenon was observed. The phase with comparatively lower resistance to actuate often surrounded the other phase while mixing. Such interfacial phenomenon needs to be studied further, since it would be important for any two or more phase separation applications on EWOD microfluidic devices, such as aqueous two-phase systems (ATPS). Almost all the dye color was extracted to the IL drop within 2−4 min while mixing.

The next step is to separate the two phases, which is a critical part of this microextraction device. To our knowledge, this is the first report on separating two immiscible droplets on a microfluidic device. Cutting a liquid drop into two droplets has been studied previously by different research groups.[39−41] To cut a liquid drop using electrowetting forces, the drop should be elongated by wetting at two ends and keeping the middle electrodes nonactivated (0 V) so that the liquid will flow to the wetted area and a neck is formed at the middle. Instead of a single phase, this study attempted cutting a drop formed by two liquid phases. As the two liquid phases have different interfacial properties, the surface tensions, the pressure differences at the interfaces, are usually different. Consequently, the two phases move at different velocities. Therefore, moving two phases onto two separate electrodes requires an intuitive way of activating the electrodes. From multiple trials it was found that the slower phase should be moved first and located on the desired electrode. Once the two phases are placed on two opposite electrodes as shown in Figure 2f and also as explained in the Experimental Section, applying a sudden impulsive potential by turning the electrodes on and off simultaneously causes phase separation. The most important observation was that the merged body tends to break into two equal volumes rather than breaking at the interface of the two phases; hence, the successful separation (without any residues from each other liquid phase) of two phases depends on the relative volumes of the two phases. When either the extractant or the donor droplet is slightly larger in volume than the other, separation creates some residue in the droplet of smaller volume. According to these observations, separation of these two particular liquid phases seems to be similar to dividing a single-phase parent droplet into two daughter droplets. Thus, it has been shown that two merged immiscible liquid drops, after a liquid−liquid extraction with 1:1 donor-to-extract volume ratio, could be successfully separated on the EWOD device. Some reports have indicated that droplet movement is biased toward an electrode activated with a higher voltage compared to the voltages applied on surrounding electrodes.[41] In addition, we know that initially droplets are

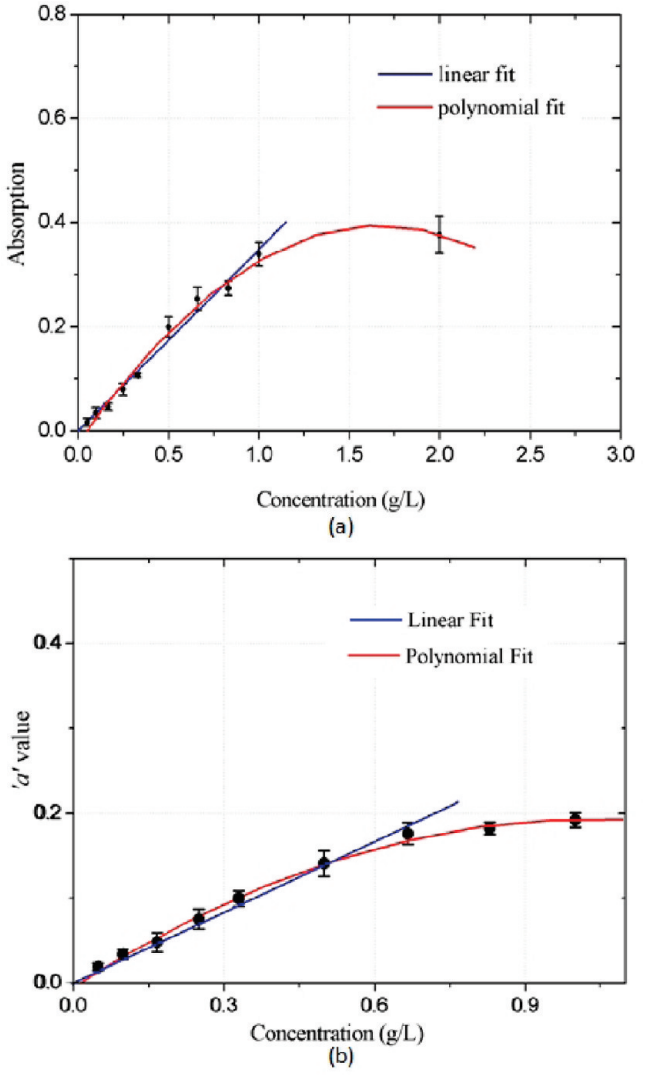

Figure 4. Comparison of calibration curves for on-chip concentration measurements: (a) UV absorption based method; (b) image-based method with "*a*" chromaticity value from the CIELab color model as the color parameter.

removed from the reservoir (larger electrode) to an actuating electrode (smaller electrode), where the volume ratio of two resultant daughter droplets seems to be dependent on the ratio of the electrode size. From these facts we can speculate that the separation of donor and extractant phases, after a microextraction of different volume ratios, may be achieved by designing different electrode sizes as well as by applying different potentials.

Real-Time Concentration Measurements. Figure 4a gives the calibration curve obtained for UV absorption based concentration measurements. The concentration range for this experiment was 0−2 g/L. The linear region for the calibration curve lies between 0 and 1 g/L. Error bars indicates the standard deviation using five data sets. The very low standard deviation (hence a higher signal-to-noise ratio) at the lowest concentration we measured indicates that the detection limit should be below 0.05 g/L.

The representation of colors in RGB is device-dependent and is a mixture of chrominance and luminance. The HSI color model defines true color by means of dominant color (*H* or hue value) and the colorfulness as a proportion of brightness (*S* or saturation) with explicit discriminations between chromaticity and luminance. The CIELab color model also defines separate measures for chrominance and luminance. Further, the CIELab model is designed to be perceptually uniform making it suitable for color comparisons. In our evaluation results, all the parameters from the RGB color model show a linear relationship with concentration in the 0−1 g/L range. Supporting Information Figure S-3 compares the variations of parameters from the three chosen color models with varying concentrations. However, the standard deviation is significant. In contrast to the RGB model, the parameters from the other two color models have very low standard deviations, even though the linear range has been limited.

The results clearly indicate the differences between the use of color models that mix chromaticity with luminance and the models that distinguish between chromaticity and luminance. When they are not distinguished, the extracted color parameters are prone to the slight illumination variations. The same ring-light with fixed illumination was used for all the experiments, as was the measured relative color change to minimize the illumination changes. However, the illumination received by different electrodes at different positions on the chip could be variable. As we did not measure the concentration of each sample keeping it on the same electrode (which is not practical), that may have led to variations in luminance and, hence, variations in the *R*, *G*, *B* parameters.

Hue (*H*) and "*a*" color components showed a very precise (low standard deviation) relationship with concentration, indicating their potential for use in concentration measurements in the microextraction device. Their best linear regions are limited to up to around 0.5 and 0.8 g/L for hue and "*a*", respectively. Among all the tested parameters the "*a*" color component gave the best plot (Figure 4b) with lowest standard deviation and a higher linear range. *H* and "*a*" components' nonlinear plots can also be used as concentration-parameter calibration curves, as long as the operating concentration range is known and is between 0 and 1 g/L. The "*b*" color component, however, does not show a significant sensitivity to concentration changes. The different sensitivities for "*a*" and "*b*" components, although they are both chromaticity values, could imply that one color range is more sensitive to the concentration. Similar effects can be observed in the RGB model, where red (*R*) parameter shows a higher sensitivity compared to the other two colors. The "*a*" color component indicates the color range from green to red, whereas the "*b*" component indicates the range from blue to yellow. UV absorbance spectrometry indicated that the solute, acid green 25, absorbs light near the red wavelengths. Therefore, it could be possible that as the concentration increases the reflected red light is decreased as the absorption increases. Red color reading in an image is the reflected light at red wavelengths, and therefore it may be giving a better relationship for color parameters that represent red color. If such a relationship exists, the color parameter that includes the color absorbed by the solute will be the best parameter to be used in image-based concentration measurement techniques.

Alternating Current Frequency Dependence of Extraction Kinetics. Figure 5 shows the decreasing pattern of donor concentration within the first 10 min for extractions that occur under five different conditions: (i) static liquid drops and no applied voltage (thus, extraction occurs naturally), (ii−iv) static liquid drop with no mixing but an ac applied voltage of 1, 10 , and 200 kHz, respectively, and (v) liquid drops with motion (mixing) under 1 kHz ac applied voltage. The decrease in donor concentration is an indication of the amount of analyte transferred to the extractant phase.

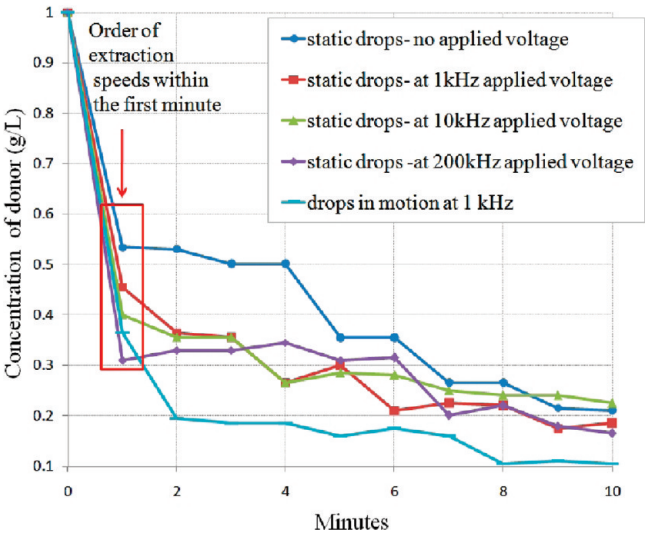

Figure 5. Frequency (of applied voltage) dependence of extraction kinetics. The highlighted rectangle in red shows the order of extraction speeds considering the first minute of the extraction process.

With an applied ac voltage (ii−iv), the donor takes less than 2 min to reach the concentration at which it took more than 5 min to reach with no applied voltage (i). This implies that frequency affects the extraction speed. When we focus on the donor concentration change within the first minute (highlighted with a red rectangle in Figure 5), it gives us a better understanding of the frequency effect. The lowest extraction speed is achieved when the droplets are static and extraction occurs naturally (i). Next, in the static drops at 1 and 10 kHz (ii and iii), the extraction is faster than in static drops with no frequency effect (i). Mixing (iv) has made the extraction even faster. However, the extraction in static drops at 200 kHz (v) seems to be the fastest, demonstrating that application of higher ac frequencies can enhance the extraction kinetics on the proposed microextraction device.

This behavior in extraction kinetics is in agreement with the previous research findings on the ac frequency effects on electrowetting. With the support of numerical simulation results, Lee et al.[24] and García-Sánchez et al.[23] reported the existence of internal flow patterns in a sessile drop under ac frequencies. As per the recent findings, flow patterns at lower frequencies (below ∼10 kHz) are caused by shape oscillations resulting from the droplet reaching its eigenfrequencies. Another strong flow pattern may evolve at higher frequencies (over ∼150 kHz) due to electrothermal or electrohydrodynamic effects induced by nonuniform electric fields and variations in the electrical properties within the drop.[23,42] Therefore, efficient mixing can be achieved by applying external ac voltages in high frequencies. Considering these findings, even though there are differences in the device format and the liquid volumes, it can be expected that there could be a nonuniform electric field at the outer curved edges of the drop. The electric field together with variations in the electrical properties due to Joule heating may lead to similar strong flows inside the sandwiched drop as well. This could explain the extraction kinetics within the first minute as a result of internal flow patterns induced by the applied ac voltage frequencies.

However, after the first minute, especially in the static drops at the 200 kHz (iv), the extraction behavior is unusual. Concentration of donor does not systematically change for the next few minutes. This must be due to the formation of satellite droplets,[43] which were observed at high frequencies. During experiment iv, such satellite droplet formation was observed (Supporting Information Figure S-4) starting after several seconds of high-frequency voltage application. Most of them did not show any dye color in them, which indicates that only water escaped from the mother drop. This droplet formation reduced the volume of the donor phase that interfaced with the extractant. It could be highly possible that the increase of donor concentration due to satellite drops is higher than the reduction in concentration due to extraction. This would explain the concentration profile at 200 kHz. At 10 kHz the donor concentration also shows less change after 5 min and may be due to similar effects. Although it is clear that higher frequencies can be used as a factor to enhance the extraction process, further work is needed to identify the exact conditions for optimal extractions.

CONCLUSION AND FUTURE WORK

A new method of liquid−liquid microextraction, which we named as DTD-LLME, was successfully achieved. The DTD-LLME provided a simplified control and complete on-chip phase separation. The separation of the merged liquid phases occurred in a similar way as breaking a single-phase mother drop into two child droplets, rather than separating at the immiscible interface. Further research with different liquid combinations as well as numerical studies will be examined subsequently.

Image-based concentration measurement methods showed the capability to precisely measure on-chip analyte concentrations, while providing more convenient and faster measurements compared to the conventional UV absorption based technique. Finally, the preliminary results reveal that the frequency of the applied ac voltage influences the extraction kinetics. At higher frequencies (>∼150 kHz), the strong internal flow patterns due to Joule heating could help mixing and influence the extraction speed in the proposed device.

When the presented on-chip DTD-LLME device is fully utilized with its multiplexing capability, it will provide a versatile sample preparation platform including high-throughput screening devices. For example, it could be used for screening task-specific ILs for various target ions or molecules.

ASSOCIATED CONTENT

Supporting Information. Additional information as noted in text. This material is available free of charge via the Internet at http://pubs.acs.org.

AUTHOR INFORMATION

Corresponding Author

*E-mail: Hyejin.moon@uta.edu. Fax: 817 272 2952.

ACKNOWLEDGMENT

Authors thank the University of Texas at Arlington Research Enhancement Program (UTA-REP) for funding this research. Furthermore, the authors thank Mr. Subin George for his support in the device fabrication process.

REFERENCES

(1) Psillakis, E.; Kalogerakis, N. *TrAC, Trends Anal. Chem.* **2003**, *22*, 565–574.
(2) Liu, H.; Dasgupta, P. K. *Anal. Chem.* **1996**, *68*, 1817–1821.
(3) Jeannot, M. A.; Cantwell, F. F. *Anal. Chem.* **1996**, *68*, 2236–2240.

(4) Pedersen-Bjergaard, S.; Rasmussen, K. E. *Anal. Chem.* **1999**, *71*, 2650–2656.
(5) Sarafraz-Yazdi, A.; Amiri, A. *TrAC, Trends Anal. Chem.* **2010**, *29*, 1–14.
(6) Wheeler, A. R. *Science* **2008**, *322*, 539.
(7) Moon, H.; Wheeler, A. R.; Garrell, R. L.; Loo, J. A.; Kim, C. J. *Lab Chip* **2006**, *6*, 1213–1219.
(8) Srinivasan, V.; Pamula, V. K.; Fair, R. B. *Anal. Chim. Acta* **2004**, *507*, 145–150.
(9) Srinivasan, V.; Pamula, V. K.; Fair, R. B. *Lab Chip* **2004**, *4*, 310–315.
(10) Srinivasan, V.; Pamula, V.; Pollack, M.; Fair, R. A Digital Microfluidic Biosensor for Multianalyte Detection. In *Proceedings of the IEEE 16th Annual International Conference on Micro Electro Mechanical Systems*, Cho, Y.-H., Tabata, O., Eds.; IEEE explore digital library: Kyoto, Japan, January 19−23, 2003; pp 327−330.
(11) Satoh, W.; Hosono, H.; Suzuki, H. *Anal. Chem.* **2005**, *77*, 6857–6863.
(12) Dubois, P.; Marchand, G.; Fouillet, Y.; Berthier, J.; Douki, T.; Hassine, F.; Gmouh, S.; Vaultier, M. *Anal. Chem.* **2006**, *78*, 4909–4917.
(13) Abdelgawad, M.; Freire, S. L. S.; Yang, H.; Wheeler, A. R. *Lab Chip* **2008**, *8*, 672–677.
(14) Nanayakkara, Y. S.; Perera, S.; Bindiganavale, S.; Wanigasekara, E.; Moon, H.; Armstrong, D. W. *Anal. Chem.* **2010**, *82*, 3146–3154.
(15) Soukup-Hein, R. J.; Warnke, M. M.; Armstrong, D. W. *Annu. Rev. Anal. Chem. (Palo Alto, Calif.)* **2009**, *2*, 145–168.
(16) Anderson, J. L.; Armstrong, D. W.; Wei, G. T. *Anal. Chem.* **2007**, *79*, 4247–4247.
(17) Meindersma, W. G.; Podt, A. J. G.; Meseguer, M. G.; de Haan, A. B. *ACS Symp. Ser.* 2005, *902*, 57–71.
(18) Yang, Q.; Xing, H.; Cao, Y.; Su, B.; Yang, Y.; Ren, Q. *Ind. Eng. Chem. Res.* **2009**, *48*, 6417–6422.
(19) Wanigasekara, E.; Perera, S.; Crank, J. A.; Sidisky, L.; Shirey, R.; Berthod, A.; Armstrong, D. W. *Anal. Bioanal Chem.* **2010**, *396*, 511–524.
(20) Aguilera-Herrador, E.; Lucena, R.; Cardenas, S.; Valcarcel, M. *Anal. Chem.* **2008**, *80*, 793–800.
(21) Yao, C.; Pitner, W. R.; Anderson, J. L. *Anal. Chem.* **2009**, *81*, 5054–5063.
(22) Baret, J.; Decré, M. M. J.; Mugele, F. *Langmuir* **2007**, *23*, 5173–5179.
(23) García-Sánchez, P.; Ramos, A.; Mugele, F. *Phys. Rev. E* **2010**, *81*, 015303–015303.
(24) Lee, H.; Yun, S.; Ko, S. H.; Kang, K. H. *Biomicrofluidics* **2009**, *3*, 44113.
(25) Malk, R.; Fouillet, Y.; Davoust, L. *Procedia Chem.* **2009**, *1*, 1107–1110.
(26) Oh, J. M.; Ko, S. H.; Kang, K. H. *Langmuir* **2008**, *24*, 8379–8386.
(27) Carda-Broch, S.; Berthod, A.; Armstrong, D. W. *Anal. Bioanal. Chem.* **2003**, *375*, 191–199.
(28) Li, C.; Xin, B.; Xu, W.; Zhang, Q. *J. Chem. Technol. Biotechnol.* **2007**, *82*, 196–204.
(29) Jensen, M. P.; Dzielawa, J. A.; Rickert, P.; Dietz, M. L. *J. Am. Chem. Soc.* **2002**, *124*, 10664–10665.
(30) Dai, S.; Ju, Y.H.; Barnes, C.E. *J. Chem. Soc., Dalton Trans.* **1999**, 1201–1202.
(31) Visser, A. E.; Swatloski, R. P.; Reichert, W. M.; Mayton, R.; Sheff, S.; Wierzbicki, A.; Davis; James, H.; Rogers, R. D. *Environ. Sci. Technol.* **2002**, *36*, 2523–2529.
(32) Asmare, M. H.; Asirvadam, V. S.; Iznita, L. Color Space Selection for Color Image Enhancement Applications. In *Proceedings of the 2009 International Conference on Signal Acquisition and Processing*; Bhadra Chaudhur, S. R., Raymond, Z.; Musumbu, K., Eds.; IEEE explore digital library: Kuala Lumpur, April 3−5, 2009; pp 208−212.
(33) Jones, T. B.; Fowler, J. D.; Chang, Y. S.; Kim, C. *Langmuir* **2003**, *19*, 7646–7651.
(34) Chatterjee, D.; Shepherd, H.; Garrell, R. L. *Lab Chip* **2009**, *9*, 1219–1229.
(35) Mugele, F.; Baret, J. C. *J. Phys.: Condens. Matter* **2005**, *17*, R705–R774.
(36) Yoon, J.; Garrell, R. L. *Anal. Chem.* **2003**, *75*, 5097–5102.
(37) Luk, V. N.; Mo, G. C. H.; Wheeler, A. R. *Langmuir* **2008**, *24*, 6382–6389.
(38) Cahill, B. P.; Giannitsis, A. T.; Land, R.; Gastrock, G.; Pliquett, U.; Frense, D.; Min, M.; Beckmann, D. *Sens. Actuators, B* **2010**, *144*, 380–386.
(39) Cho, S. K.; Moon, H.; Kim, C. J. *J. Microelectromech. Syst.* **2003**, *12*, 70–80.
(40) Jang, L. S.; Lin, G. H.; Lin, Y. L.; Hsu, C. Y.; Kan, W. H.; Chen, C. H. *Biomed. Microdevices* **2007**, *9*, 777–786.
(41) Walker, S. W.; Shapiro, B. *J. Microelectromech. Syst.* **2006**, *15*, 986–1000.
(42) Ko, S. H.; Lee, H.; Kang, K. H. *Langmuir* **2008**, *24*, 1094–1101.
(43) Hong, J. S.; Ko, S. H.; Kang, K. H.; Kang, I. S. *Microfluid. Nanofluid.* **2008**, *5*, 263–271.